prosthesis

MDPI

Article

Novel Reverse Zygomatic Implant Approach: Expanded Cadaveric Validation, Surgical Accuracy, and Comparison of Orbital Access Routes—Part 2

Ada Ferrer-Fuertes [1,2,*], Francisco Javier Cuesta-González [1], Ramón Sieira-Gil [1], Samir Aboul-Hosn-Centenero [1], Eloy García-Díez [1], Alberto Prats-Galino [2], Laura Pozuelo-Arquimbau [1], Pau Rodriguez-Berart [1], Irene Vila-Masana [1] and Carles Marti-Pagés [1,*]

[1] Maxillofacial Surgery Department, Clinic Hospital, C/Villarroel 170, 08014 Barcelona, Spain; fjcuesta@clinic.cat (F.J.C.-G.); rsieira@clinic.cat (R.S.-G.); saboul@clinic.cat (S.A.-H.-C.); emgarcia@clinic.cat (E.G.-D.); lpozueloa@clinic.cat (L.P.-A.); rodriguezs@clinic.cat (P.R.-B.); ivilam@clinic.cat (I.V.-M.)

[2] Laboratory of Surgical Neuroanatomy (LSNA), Faculty of Medicine & Health Sciences, Universitat de Barcelona, C/Casanova 143, 08036 Barcelona, Spain; aprats@ub.edu

* Correspondence: ferrer@clinic.cat (A.F.-F.); cmarti1@clinic.cat (C.M.-P.)

Abstract

Background: Conventional zygomatic implant placement may be technically impossible in patients with severe trismus or extensive post-maxillectomy defects because adequate intraoral access is required. This study evaluated the feasibility, accuracy, anatomical safety, and prosthetic correspondence of a novel reverse zygomatic implant inserted from the zygomatic surface toward the oral cavity. **Materials and Methods:** Nine fresh-frozen cadaveric heads underwent simulated Brown Class II maxillectomies. Thirty-six reverse zygomatic implants were virtually planned at positions 13, 15, 23, and 25 and placed using specimen-specific CAD/CAM drilling guides. A superior blepharoplasty approach and an inferior transconjunctival approach with lateral canthotomy and cantholysis were evaluated. Postoperative CT superimposition was used to measure linear and angular deviations. Zygomatic bone volume, implant trajectory, primary stability, complications, and correspondence with a specimen-specific polyamide verification bar were also assessed. **Results:** Thirty-five of the 36 implants achieved primary stability, corresponding to a technical success rate of 97.2%. Mean deviation was 2.22 ± 1.41 mm at the zygomatic entry point and 4.41 ± 1.82 mm at the intraoral emergence point. Mean angular deviation was 3.83 ± 1.71°. No statistically significant differences were identified according to implant position, laterality, surgical access route or zygomatic bone volume. Two anterior zygomatic cortical fractures occurred; one resulted in loss of primary stability. No orbital or infratemporal penetration was observed. Complete prosthetic correspondence was obtained at a median of two of the four abutments per specimen, and none of the verification bars achieved complete passive seating over all four abutments. **Conclusions:** Guided reverse zygomatic implant placement was technically feasible and reproducible regarding implant stability in this cadaveric model. However, cortical fracture risk and incomplete prosthetic correspondence indicate that further optimization and prospective clinical validation are required before routine clinical application.

Keywords: reverse zygomatic implant; maxillectomy; trismus; guided implant surgery; zygomatic implants; CAD/CAM surgical guides; placement accuracy; prosthetic rehabilitation

Check for updates

Academic Editor: Marco Cicciu

Received: 13 August 2026
Revised: 20 September 2026
Accepted: 22 September 2026
Published: 27 September 2026

Copyright: © 2026 by the authors. Licensee MDPI, Basel, Switzerland. This article is an open access article distributed under the terms and conditions of the Creative Commons Attribution (CC BY) license.

1. Introduction

Dental rehabilitation after maxillectomy remains a major clinical challenge. Loss of the maxillary dentition and supporting tissues may severely affect mastication, swallowing, speech, facial appearance, and quality of life [1,2]. Although obturator prostheses and reconstructive surgery can restore some anatomical and functional components, adequate prosthetic retention may be difficult to achieve in patients with extensive defects, limited residual dentition, xerostomia, postoperative scarring, or altered maxillary anatomy [1,3].

Zygomatic implants provide an alternative anchorage site when the residual maxillary bone is insufficient for conventional dental implants [4,5]. Their use has been extended from the rehabilitation of severely atrophic maxillae to patients who have undergone oncological maxillectomy or complex maxillary reconstruction [3,6,7]. Computer-assisted planning and patient-specific surgical guides are particularly valuable in these cases because conventional anatomical landmarks may be absent, displaced, or covered by reconstructive soft-tissue flaps [6–8].

Nevertheless, conventional zygomatic implant placement requires the introduction of long drills and implants from the oral cavity toward the zygomatic bone. Adequate mouth opening is therefore necessary for visualization, instrumentation, irrigation, surgical guidance, and protection of the surrounding tissues. Patients previously treated for head and neck cancer frequently present with trismus caused by surgical scarring, radiotherapy-induced fibrosis, or combined chemoradiotherapy [9,10]. In severe cases, the zygomatic bone may remain suitable for anchorage even though conventional intraoral implant insertion is technically impossible.

To overcome this limitation, Dawood et al. described the reverse insertion of a zygomatic implant from the external surface of the zygoma toward the oral cavity [11]. However, the initial report represented an individualized application and did not establish a standardized implant design, reproducible surgical workflow, or quantitative assessment of placement accuracy.

In Part 1 of the present research program, our group introduced a specifically designed reverse zygomatic implant and a digitally planned, guide-assisted surgical protocol [12]. Four implants were placed in a fresh-frozen cadaveric specimen in which a Brown Class II maxillectomy defect was reproduced. The procedure demonstrated initial technical feasibility, primary stability, preservation of the relevant anatomical structures, and intraoral emergence positions potentially compatible with prosthetic rehabilitation. Postoperative three-dimensional analysis also showed that small deviations at the zygomatic entry point could become magnified at the intraoral emergence because of the extended implant trajectory.

The present Part 2 study therefore expands the initial investigation to nine fresh-frozen cadaveric heads, comprising the original proof-of-concept specimen and eight additional specimens treated using the same reverse-insertion principle with a total of 36 implants to evaluate the reproducibility of the technique across different anatomical conditions.

2. Materials and Methods

2.1. Study Design and Ethical Approval

An experimental cadaveric study was conducted using nine fresh-frozen human cadaveric heads to evaluate the feasibility, anatomical safety, and positional accuracy of a reverse zygomatic implant system. The study expanded the proof-of-concept protocol described in Part 1 and included the original specimen and eight additional specimens treated using the same reverse-insertion principle [12].

The procedures were performed under laboratory conditions reproducing standard maxillofacial surgical practice. Ethical approval was obtained from the Ethics Committee of

the University of Barcelona (IRB00003099; approval date: 28 February 2022). All specimens were obtained through the institutional body donation program. The donors had provided premortem consent for the use of their bodies for educational and research purposes. All procedures complied with the applicable institutional regulations governing anatomical donation and cadaveric research.

2.2. Experimental Maxillectomy Model

A Brown Class II maxillectomy defect was reproduced in each specimen to simulate the anatomical conditions encountered after low-level maxillectomy [13]. Before surgery, the maxillectomy osteotomies were virtually planned and transferred to the specimens using patient-specific CAD/CAM cutting guides.

One or more maxillary anterior teeth were preserved during creation of the defect. These teeth served as reproducible anatomical references for alignment of the preoperative and postoperative computed tomography datasets and for evaluation of the intraoral emergence positions. They were removed only after completion of the radiological assessment when required for placement of the prosthetic verification bar.

2.3. Reverse Zygomatic Implant Design

The reverse zygomatic implant used in this study was previously introduced and described in detail in Part 1 [12]. Briefly, it was specifically designed for retrograde insertion from the external surface of the zygomatic bone toward the oral cavity.

The implant comprised two functionally distinct segments (Figure 1):

1. A polished, non-threaded passive stem designed to pass through the zygomatic bone and adjacent soft tissues with minimal friction.
2. A 20 mm active threaded segment designed to obtain bicortical anchorage within the zygomatic bone and provide primary mechanical stability.

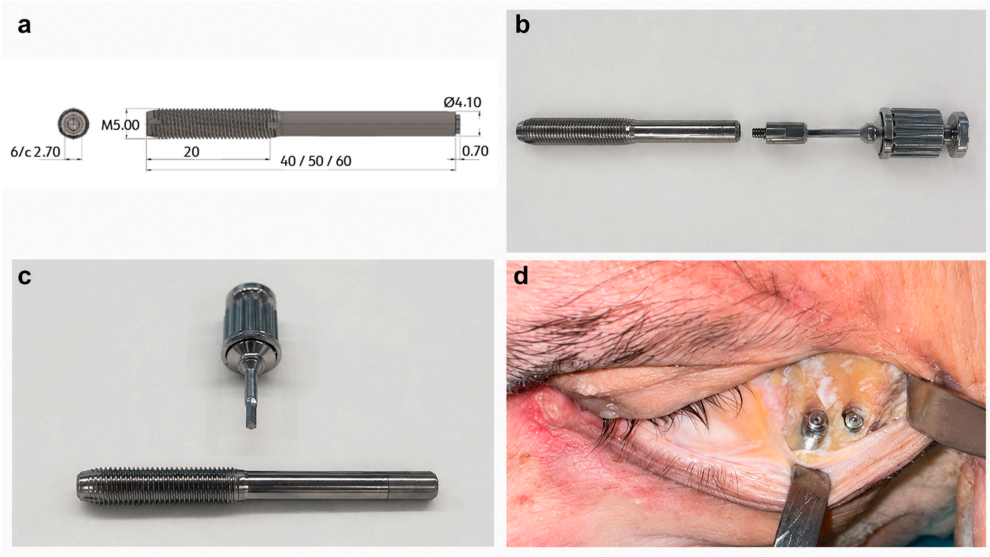

Figure 1. Reverse zygomatic implant design and system components. (**a**) Technical design of the reverse zygomatic implant, comprising an active threaded segment intended for zygomatic anchorage and a polished passive stem directed toward the oral cavity. (**b**) Implant assembled with the transport connector and insertion driver. (**c**) Alignment of the components before engagement. (**d**) External cover caps positioned over the zygomatic ends of the implants.

The implants were manufactured from titanium alloy Grade 23 ELI (Ti6Al4V). The diameter ranged from 4.1 mm at the passive stem to 5.0 mm at the active threaded segment. Three implant lengths—40, 50, and 60 mm—were available and selected according to

the virtually planned distance between the external zygomatic surface and the intended intraoral emergence position.

A removable external transport carrier was connected to the intraoral end to control implant insertion and orientation. After final seating, the carrier was removed, and a 30° angled transepithelial abutment with a 4.1 mm prosthetic connection was attached. A cover cap was placed at the external zygomatic end to limit soft-tissue ingrowth into the implant connection.

2.4. Computed Tomography and Virtual Surgical Planning

Each specimen underwent a preoperative high-resolution maxillofacial CT scan using a Siemens Somatom Go.Top 64-slice scanner with version VA40A software (Siemens Healthineers, Forchheim, Germany). Images were acquired using a slice thickness of 0.6 mm and exported in Digital Imaging and Communications in Medicine (DICOM) format.

The DICOM datasets were processed using Mimics Medical 26.0 for segmentation and 3-Matic Medical 18.0 for three-dimensional planning and design (Materialise, Leuven, Belgium). The maxillary and zygomatic bones, orbital boundaries, residual dentition, and relevant adjacent anatomical structures were segmented.

Four reverse zygomatic implants were planned for each specimen. The intended intraoral emergence positions corresponded to the maxillary canine and second premolar regions:

- Z1: position 13.
- Z2: position 15.
- Z3: position 23.
- Z4: position 25.

Implant trajectories were adjusted in the axial, sagittal, and coronal planes to maximize engagement of the zygomatic bone while avoiding the orbit, infraorbital region, maxillary sinus where anatomically possible, and infratemporal fossa (Figure 2). Prosthetically favorable intraoral emergence and adequate separation between implants were considered during planning.

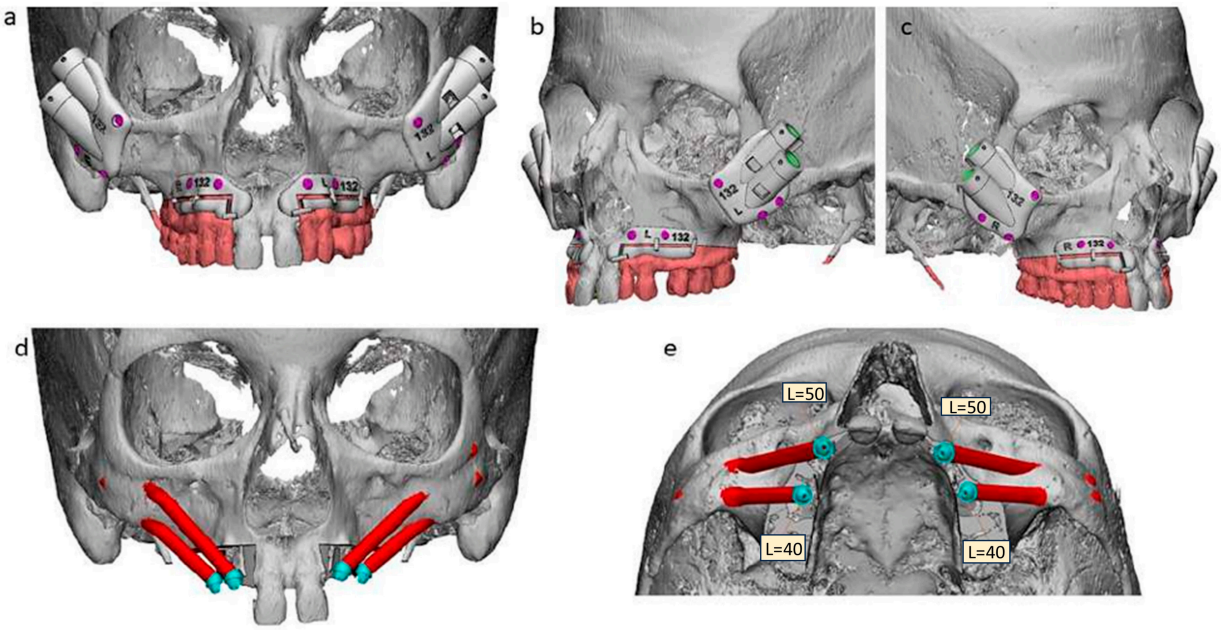

Figure 2. Virtual surgical planning and specimen-specific guide design. (**a**) Virtual simulation of the Brown Class II maxillectomy and design of the specimen-specific cutting guides. (**b**,**c**) Design and positioning of the zygomatic-supported drilling guides. (**d**,**e**) Planned reverse zygomatic implant trajectories extending from the external zygomatic surface toward the intraoral emergence sites.

2.5. Design and Manufacturing of the Surgical Guides

Two patient-specific guide systems were designed for each specimen (Figure 2):

1. A maxillectomy cutting guide to reproduce the planned Brown Class II defect.
2. Bilateral zygomatic drilling guides to transfer the virtually planned implant trajectories to the exposed zygomatic surfaces.

The guides were manufactured from biocompatible polyamide PA 2200 using a Formiga P110 selective laser-sintering system (EOS GmbH, Krailling, Germany). Each maxillectomy cutting guide was designed to adapt to the maxillary bony contour and was secured using three titanium fixation screws (Titamed, Kontich, Belgium).

2.6. Surgical Access Routes

Two different approaches to the zygomatic surface were evaluated within each specimen:

- A superior blepharoplasty incision with lateral extension on one side.
- An inferior transconjunctival approach with lateral canthotomy and cantholysis on the contralateral side.

The side allocated to each approach varied between specimens. Both approaches were extended laterally as required to expose the zygomatic surface and permit positioning, fixation, and use of the drilling guides.

The length of the lateral extension was measured from the lateral canthus to the lateral limit of the incision. Surgical exposure was assessed according to the visibility of the zygomatic surface, available working space, ease of guide adaptation, guide fixation, and accessibility for drilling and implant insertion.

2.7. Drilling and Implant Placement

The drilling guides were positioned on the exposed zygomatic surfaces and secured with three titanium screws (Titamed, Kontich, Belgium). Sequential osteotomy preparation was performed using commercially available zygomatic implant drills from Southern Implants (Irene, South Africa), Straumann (Basel, Switzerland), and Avinent Implant System (Santpedor, Spain).

Guide adaptation, stability, accessibility, and visibility of the drilling field were assessed intraoperatively.

Drilling was performed at low rotational speed under continuous irrigation with sterile 0.9% sodium chloride solution. The preparation sequence was adapted to the planned implant diameter because a dedicated drilling system for the reverse implant prototype was not available.

After completion of the osteotomy, each implant was inserted from the external zygomatic surface toward the planned intraoral emergence point. Initial insertion was performed at 20–40 rpm, with a target insertion torque of up to 40 N·cm. Final seating and orientation were completed manually.

The external transport carrier was subsequently removed, and a 30° angled transepithelial abutment was connected at the intraoral end. The abutments were oriented to obtain the greatest possible parallelism and facilitate connection to the planned prosthetic structure. A cover cap was then placed at the zygomatic end.

2.8. Primary Stability and Anatomical Safety

Primary implant stability was assessed manually after final seating by the same surgeon in all cases (C.M.-P.). Lack of primary stability was defined as detectable rotational movement when a torque of 35 N·cm was applied using a manual torque wrench.

The specimens were inspected for procedure-related complications, including:

- Fracture of the anterior or lateral zygomatic cortical wall.
- Orbital penetration.
- Entry into the infratemporal fossa.
- Unintended sinus penetration.
- Damage to the infraorbital region.
- Soft-tissue perforation.
- Loss of primary implant stability.

Implant placement was considered technically successful when the implant reached the planned general trajectory, maintained primary stability, and did not require removal because of a procedure-related complication.

2.9. Postoperative CT and Three-Dimensional Accuracy Assessment

After placement of the four implants, a postoperative CT scan was obtained using the same scanner and acquisition parameters as the preoperative examination. The preoperative virtual plan and postoperative CT reconstruction were aligned using the preserved teeth and stable craniofacial anatomical structures as registration references.

Three-dimensional superimposition was performed using Mimics Medical 26.0 and 3-Matic Medical 18.0. The planned and achieved implant positions were compared using the following measurements:

1. Zygomatic linear deviation: three-dimensional distance between the planned and achieved implant positions at the zygomatic entry point.
2. Intraoral linear deviation: three-dimensional distance between the planned and achieved positions at the intraoral emergence point.
3. Angular deviation: angle between the longitudinal axes of the planned and achieved implants.

Deviations were analyzed according to implant position, surgical access route, and laterality.

2.10. Zygomatic Bone and Implant Trajectory Assessment

The volume of each zygomatic bone was calculated from the segmented preoperative CT dataset and expressed in cubic centimeters. The relationship between available zygomatic bone volume and implant placement deviation was explored separately for each side.

The proportion of each implant trajectory located outside the segmented zygomatic bone was calculated as an exploratory anatomical variable. Implant trajectories were also classified according to their relationship with the maxillary sinus using the zygoma anatomy-guided approach classification [14].

2.11. Prosthetic Verification

A patient-specific polyamide verification bar resembling an Ackermann-type prosthetic framework was designed according to the planned intraoral emergence positions. After postoperative imaging and removal of the remaining reference teeth when necessary, the bar was positioned over the four transepithelial abutments.

For each implant, prosthetic correspondence was classified according to whether the abutment achieved complete seating with the corresponding opening in the verification bar. The number of fully matching abutments was recorded for each specimen. Partial contact or inability to seat the bar completely was documented separately.

This binary assessment replaced the preliminary system based on variable numbers of "+" symbols, providing a more reproducible evaluation of prosthetic correspondence.

2.12. Outcome Measures

The primary outcomes were:

- Successful placement of the reverse zygomatic implants.
- Zygomatic, intraoral, and angular deviations from the virtual plan.
- Maintenance of primary implant stability.
- Absence of damage to critical anatomical structures.

Secondary outcomes included:

- Differences in placement accuracy between the two surgical access routes.
- Influence of implant position and laterality on placement accuracy.
- Association between zygomatic bone volume and implant deviation.
- Prosthetic correspondence with the verification bar.
- Incidence and characteristics of procedure-related complications.

2.13. Statistical Analysis

Categorical variables were expressed as frequencies and percentages. Continuous variables were described as mean and standard deviation or as median and range, depending on their distribution. Normality was evaluated using the Shapiro–Wilk test.

Because four implants were placed within each specimen, implant-level observations were considered correlated. The influence of implant position on zygomatic, intraoral, and angular deviations was evaluated using repeated-measures analysis of variance. When the assumptions required for parametric analysis were not satisfied, the corresponding non-parametric repeated-measures test was applied.

For comparison of the superior and inferior approaches, the mean deviation of the two implants placed through each approach was calculated for every specimen. These specimen-level paired measurements were compared using a paired-samples *t*-test or Wilcoxon signed-rank test, according to data distribution. The same paired approach was used to evaluate laterality.

The association between zygomatic bone volume and placement deviation was assessed using Spearman's rank correlation coefficient. Statistical analyses were conducted using R software, version 4.3.1. All tests were two-sided, and statistical significance was established at $p < 0.05$.

3. Results

3.1. Procedural Feasibility

Nine fresh-frozen cadaveric heads underwent bilateral reverse zygomatic implant placement. The number of specimens was determined by anatomical availability. A total of 36 implants were inserted: 18 anterior implants at positions 13 and 23 and 18 posterior implants at positions 15 and 25. Complete postoperative CT and three-dimensional accuracy data were available for all implants.

The virtual planning workflow, simulated Brown Class II maxillectomy, planned implant trajectories, and specimen-specific cutting and drilling guides are presented in Figure 2.

Thirty-five of the 36 implants fulfilled the predefined criteria for technical success, corresponding to a procedural success rate of 97.2% (95% confidence interval: 85.5–99.9%). One implant failed to achieve primary stability following fracture of the anterior zygomatic cortical wall.

The median implant length was 50 mm for the anterior positions and 40 mm for the posterior positions. Overall, 13 implants measured 40 mm, 18 measured 50 mm, and five measured 60 mm (Table 1).

Table 1. Procedural characteristics of reverse zygomatic implant placement. The table presents the preserved maxillary teeth, surgical access route assigned to each side, implant lengths according to the FDI two-digit notation (positions 13, 15, 23, and 25) and lateral incision extension from the lateral canthus to the lateral límit of the incision. R: right; L: left.

Specimen	Preserved Maxillary Teeth	Implant Length (mm)				Superior Approach		Inferior Approach	
		13	15	23	25	Side	Lateral Extension (mm)	Side	Lateral Extension (mm)
1	11-21	50	40	50	40	R	25	L	27
2	11-21	50	40	50	40	R	23	L	20
3	11-12-21-22	60	50	60	50	L	30	R	25
4	11	50	40	50	40	R	28	L	26
5	11-21	50	40	50	40	R	27	L	30
6	22	50	40	50	40	L	22	R	20
7	11-21	50	40	50	40	R	30	L	30
8	11-21	60	50	60	50	L	25	R	30
9	11-21	50	40	50	40	R	21	L	23

Both surgical approaches provided sufficient exposure of the zygomatic surface to position and secure the drilling guides. The mean lateral extension of the incision was 25.7 mm for both approaches, ranging from 21 to 30 mm for the superior blepharoplasty approach and from 20 to 30 mm for the inferior transconjunctival approach (Table 1).

All planned osteotomies were successfully completed after guide fixation. In some specimens, additional preparation of the external zygomatic cortex was required to accommodate the diameter of the implant carrier. Reverse insertion from the zygomatic surface toward the oral cavity was completed at all 36 planned implant sites. Final seating and connection of the transepithelial abutments were achieved in 35 implants with primary stability.

3.2. Zygomatic Anatomy and Implant Trajectory

The median zygomatic bone volume was 4.06 cm^3, ranging from 2.53 to 8.10 cm^3. The median volume was 4.04 cm^3 on the right side and 4.12 cm^3 on the left side (Table 2).

Table 2. Zygomatic bone volume and proportion of the planned implant trajectory located outside the segmented zygomatic bone. Bone volume is reported separately for the right and left zygomatic bones. The proportion of the trajectory located outside the bone is presented for implant positions 13, 15, 23, and 25. Thirty–four of 36 trajectories (94.4%) were classified as ZAGA III–IV.

Specimen	Zygomatic Bone Volume (cm^3)		Implant Trajectory Outside The Bone (%)			
	Right	Left	13	15	23	25
1	4.08	4.65	68.22	79.96	78.51	79.62
2	4.04	4.12	61.66	53.84	69.18	71.56
3	3.99	3.76	67.90	67.39	74.42	64.36
4	3.25	2.90	60.64	75.28	66.80	70.04
5	3.31	3.49	60.78	73.72	71.87	60.78
6	4.29	4.82	63.78	67.05	67.21	69.51
7	6.30	6.70	69.86	64.72	72.70	64.95
8	2.69	2.53	67.33	74.87	75.37	74.48

Table 2. *Cont.*

Specimen	Zygomatic Bone Volume (cm^3)		Implant Trajectory Outside The Bone (%)			
	Right	Left	13	15	23	25
9	8.10	7.6	79.38	51.91	69.33	60.63
Summary	4.04	4.12	66.62	67.64	71.71	68.44

Thirty-four of the 36 implant trajectories (94.4%) followed an extrasinusal pathway corresponding to ZAGA III or IV anatomy [14]. The mean proportion of the implant trajectory located outside the segmented zygomatic bone was 68.6% ± 6.8%, ranging from 51.91% to 79.96%.

According to implant position, the mean proportions of the implant trajectory located outside the zygomatic bone were 66.62% at position 13, 67.64% at position 15, 71.71% at position 23, and 68.44% at position 25 (Table 2).

3.3. Three-Dimensional Placement Accuracy

Postoperative CT reconstruction and superimposition onto the preoperative virtual plan were successfully completed for all nine specimens (Figure 3).

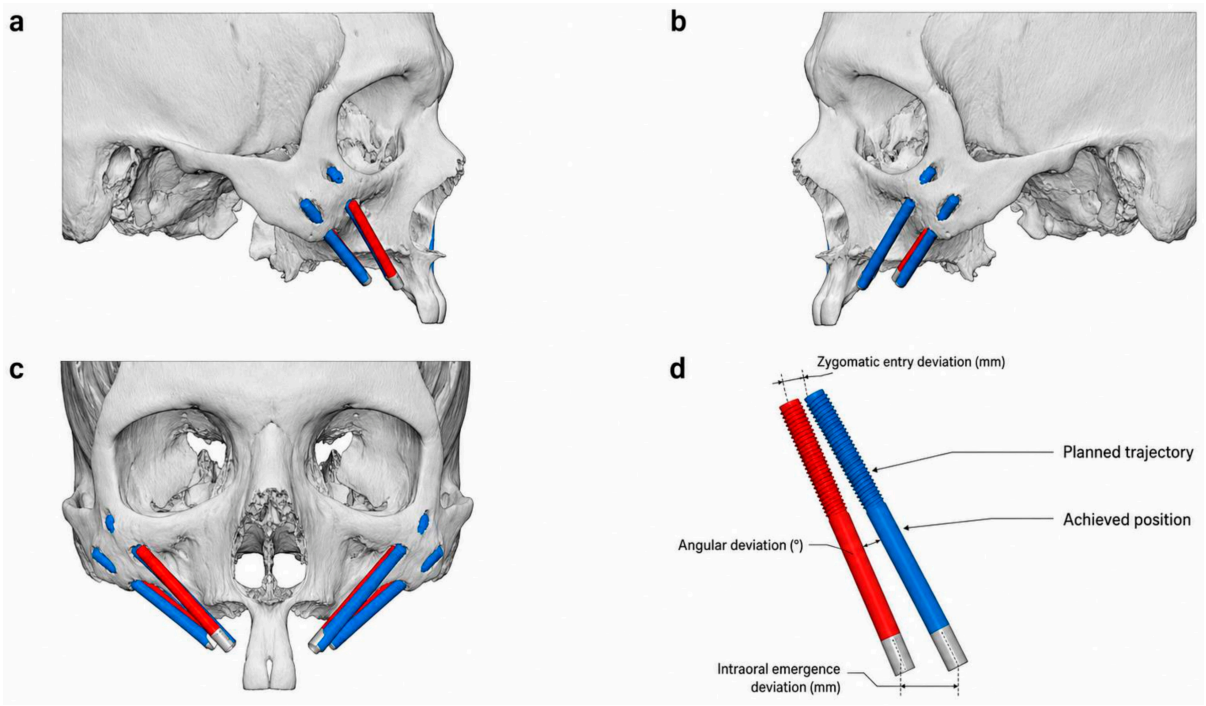

Figure 3. Three-dimensional comparison between the planned and achieved reverse zygomatic implant positions. (**a**–**c**) Representative postoperative computed tomography reconstructions showing superimposition of the planned implant trajectories (red) and the achieved implant positions (blue). (**d**) Measurement method used to calculate the linear deviation at the zygomatic entry point, linear deviation at the intraoral emergence point, and angular deviation between the planned and achieved implant axes.

The mean linear deviation at the zygomatic entry point was 2.22 ± 1.41 mm, with a median of 2.10 mm and a range of 0.36–5.64 mm.

The mean linear deviation at the intraoral emergence point was 4.41 ± 1.82 mm, with a median of 4.41 mm and a range of 1.23–8.95 mm. Thus, the observed deviation was numerically greater at the intraoral emergence point than at the zygomatic entry point.

The mean angular deviation between the planned and achieved implant axes was 3.83° ± 1.71°, with a median of 3.98° and a range of 0.65–7.30°.

The complete distribution of zygomatic, intraoral, and angular deviations for each of the 36 implants is presented in Figure 4.

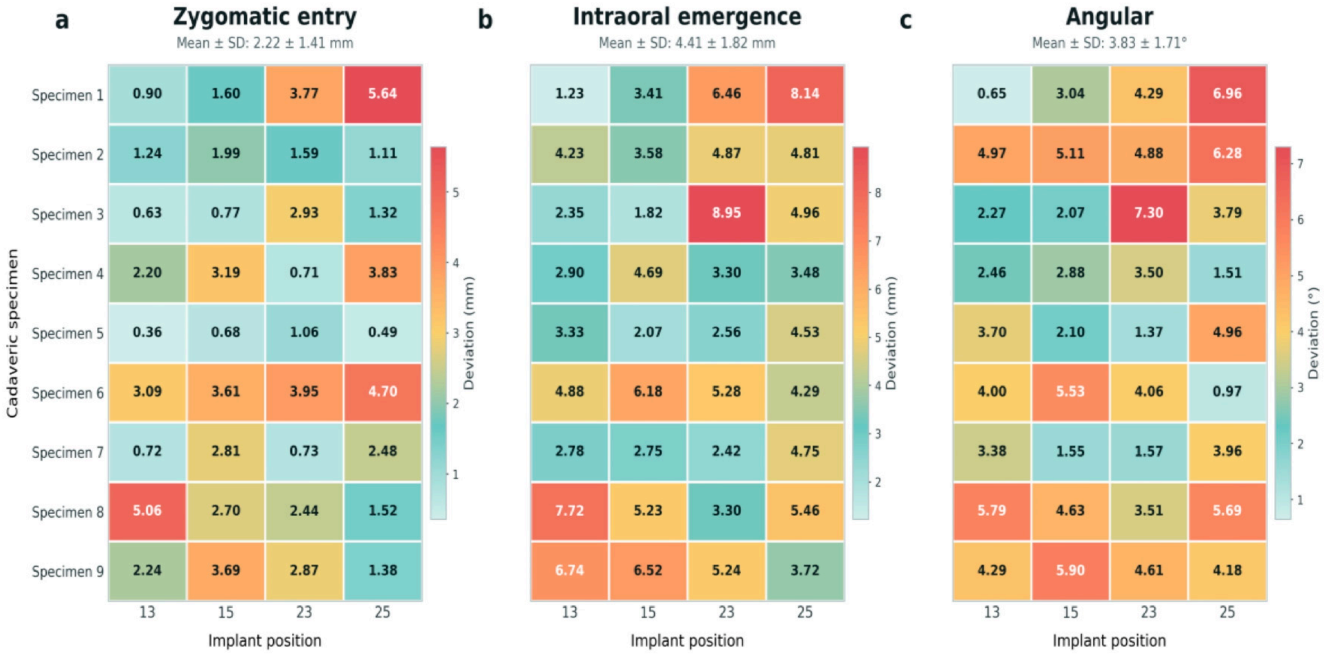

Figure 4. Distribution of three-dimensional placement deviations across specimens and implant positions. Heatmaps show the linear deviation at the zygomatic entry point, linear deviation at the intraoral emergence point, and angular deviation for each of the 36 reverse zygomatic implants. Rows represent the nine cadaveric specimens, and columns represent implant positions 13, 15, 23, and 25. The color scale indicates the magnitude of each deviation.

3.4. Accuracy According to Implant Position

The mean deviation at the zygomatic entry point was 1.83 ± 1.52 mm at position 13, 2.34 ± 1.14 mm at position 15, 2.23 ± 1.26 mm at position 23, and 2.50 ± 1.80 mm at position 25. No statistically significant differences were observed among the four implant positions ($p = 0.694$) (Figure 4).

The mean intraoral linear deviation was 4.02 ± 2.11 mm at position 13, 4.03 ± 1.72 mm at position 15, 4.71 ± 2.11 mm at position 23, and 4.90 ± 1.36 mm at position 25.

Although the posterior implant positions showed numerically greater intraoral deviations, repeated-measures analysis demonstrated no statistically significant effect of implant position on intraoral deviation ($p = 0.649$).

The mean angular deviation was 3.50 ± 1.54° at position 13, 3.65 ± 1.66° at position 15, 3.90 ± 1.78° at position 23, and 4.26 ± 2.02° at position 25. Implant position did not significantly affect angular deviation ($p = 0.789$).

The specimen-level distributions showed that the largest deviations were not consistently associated with a particular implant position but varied among the cadaveric specimens (Figure 4).

3.5. Comparison of Surgical Access Routes

For each specimen, the mean deviation of the two implants placed through each surgical approach was calculated before the paired comparison.

The mean deviation at the zygomatic entry point was 2.31 ± 1.40 mm for the inferior transconjunctival approach and 2.14 ± 1.10 mm for the superior blepharoplasty approach. The difference was not statistically significant ($p = 0.753$).

The mean intraoral emergence deviation was 4.58 ± 1.65 mm for the inferior approach and 4.25 ± 1.66 mm for the superior approach, without a statistically significant difference ($p = 0.724$).

The mean angular deviation was 4.02 ± 1.38° for the inferior approach and 3.63 ± 1.41° for the superior approach. This difference was also not statistically significant ($p = 0.568$).

The paired comparisons of zygomatic, intraoral, and angular deviations between the two surgical access routes are presented in Figure 5. Although the inferior transconjunctival approach was subjectively considered to provide greater working space and easier guide positioning, no quantitative superiority in placement accuracy was demonstrated for either approach.

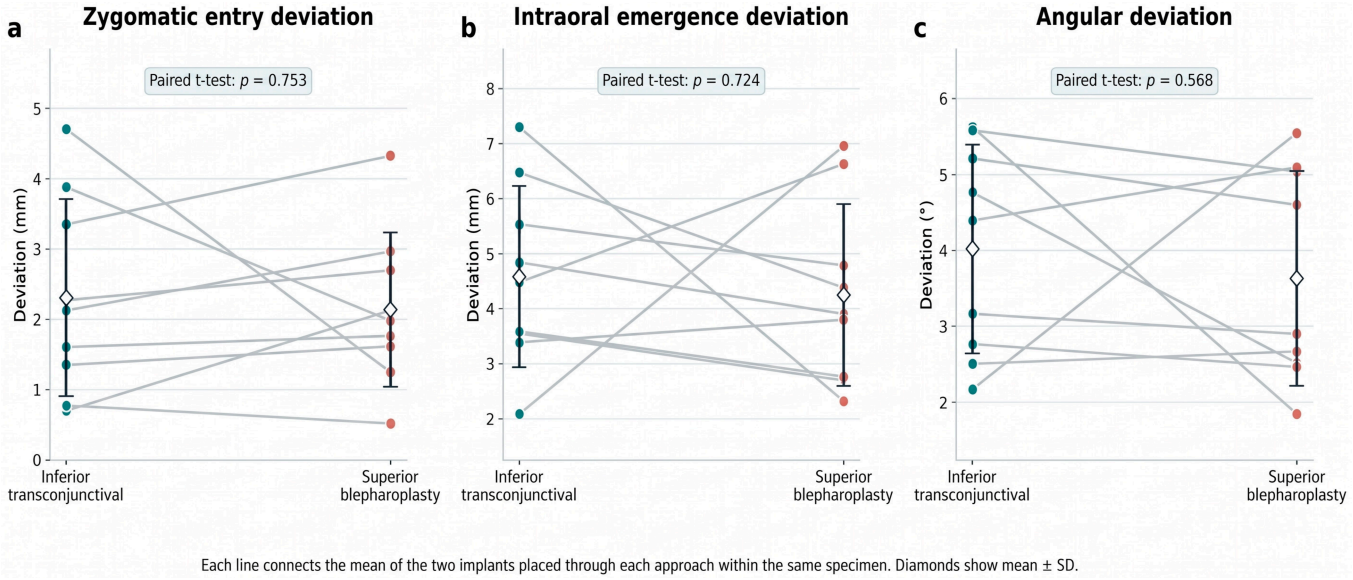

Figure 5. Paired comparison of reverse zygomatic implant placement accuracy between the inferior transconjunctival approach with lateral canthotomy and cantholysis and the superior blepharoplasty approach. Comparisons are shown for (**a**) linear deviation at the zygomatic entry point, (**b**) linear deviation at the intraoral emergence point, and (**c**) angular deviation. Each connecting line represents the paired mean measurements obtained from the same specimen, and diamonds represent the group mean ± standard deviation. No statistically significant differences were detected between the two surgical access routes using paired *t*-tests.

3.6. Accuracy According to Laterality

No statistically significant differences in placement accuracy were identified between the right and left sides.

The mean deviation at the zygomatic entry point was 2.08 ± 1.19 mm on the right side and 2.36 ± 1.31 mm on the left side ($p = 0.599$).

The mean intraoral emergence deviation was 4.02 ± 1.77 mm on the right side and 4.81 ± 1.42 mm on the left side ($p = 0.396$).

The mean angular deviation was 3.57 ± 1.51° on the right side and 4.08 ± 1.80° on the left side ($p = 0.456$). The specimen-level measurements according to implant position and laterality are shown in Figure 4.

3.7. Relationship Between Zygomatic Bone Volume and Placement Accuracy

For each side, the mean deviation of the two implants was calculated before correlation with the corresponding zygomatic bone volume.

No statistically significant correlation was identified between zygomatic bone volume and deviation at the zygomatic entry point. Spearman's correlation coefficient was ρ = 0.07 on the right side (p = 0.865) and ρ = 0.19 on the left side (p = 0.620) (Figure 6).

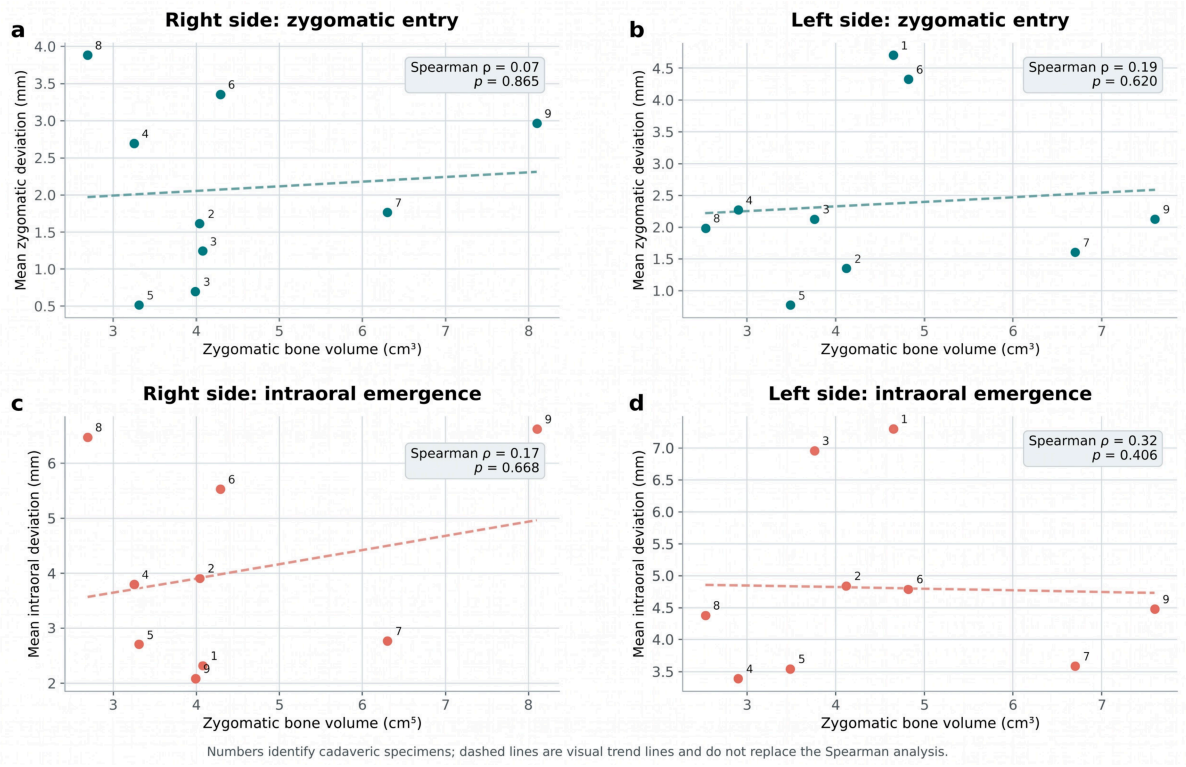

Figure 6. Relationship between zygomatic bone volume and reverse zygomatic implant placement deviation. Scatter plots show the association between zygomatic bone volume and mean deviation at the zygomatic entry point on the (**a**) right and (**b**) left sides, and between zygomatic bone volume and mean intraoral emergence deviation on the (**c**) right and (**d**) left sides. Each point represents one side of a cadaveric specimen and corresponds to the mean value of the two implants placed on that side. Correlations were evaluated using Spearman's rank correlation coefficient. No statistically significant associations were identified.

Similarly, no statistically significant association was found between zygomatic bone volume and intraoral emergence deviation. Spearman's correlation coefficient was ρ = 0.17 on the right side (p = 0.668) and ρ = 0.32 on the left side (p = 0.406) (Figure 6).

3.8. Prosthetic Verification

The specimen-specific polyamide verification bar was positioned over the four transepithelial abutments in each specimen (Figure 7). Complete correspondence was defined as complete seating of the verification bar over the corresponding abutment without a macroscopically detectable gap. Partial seating or spatial mismatch was observed at the remaining abutment positions.

Complete correspondence was recorded in a median of two abutments per specimen, with a range of two to three matching abutments. This represented a median correspondence of 50%, with a range of 50–75% (Table 3).

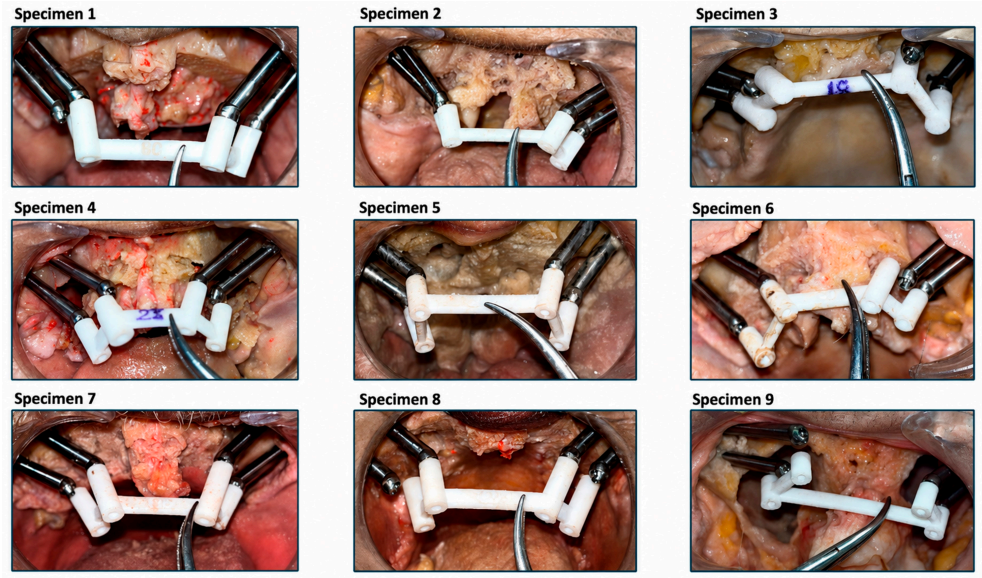

Figure 7. Representative views of the prosthetic verification using the specimen-specific polyamide bar positioned over the four transepithelial abutments in the cadaveric specimens.

Table 3. Prosthetic correspondence between the specimen-specific polyamide verification bar and the transepithelial abutments. Complete correspondence was defined as complete seating of the verification bar over the corresponding abutment without a macroscopically detectable gap. Results are reported as the number and percentage of abutments demonstrating complete correspondence in each cadaveric specimen.

Specimen	Fully Matching Abutments (n/4)	Correpondence (%)	Complete Four-Abutment Passive-Seating
1	2	50	No
2	3	75	No
3	2	50	No
4	2	50	No
5	3	75	No
6	2	50	No
7	3	75	No
8	2	50	No
9	2	50	No
Summary	Median: 2 Range: 2–3	Median: 50 Range: 50–75	0/9 specimens

Three specimens demonstrated complete correspondence at three of the four abutments, whereas six specimens demonstrated complete correspondence at two abutments. None of the nine verification bars achieved complete passive seating over all four abutments simultaneously (Table 3). Partial seating or spatial mismatch was observed at the remaining abutment positions.

3.9. Complications and Anatomical Safety

Two implants produced fractures of the anterior cortical wall of the zygomatic bone, corresponding to 5.6% of all implant placements (Figure 8).

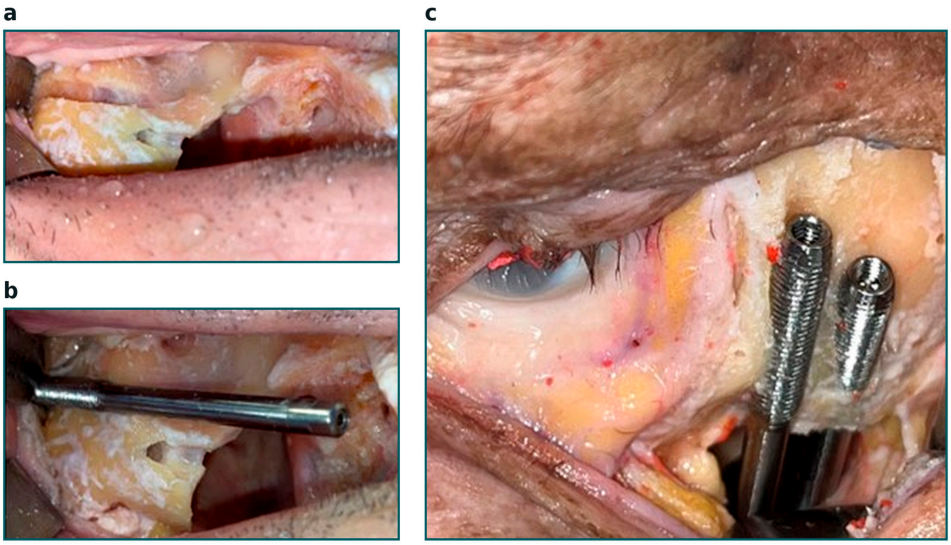

Figure 8. Fracture of the anterior zygomatic cortical wall during reverse zygomatic implant placement. (**a**,**b**) Cortical fracture observed in specimen 8, resulting in rotational mobility and loss of primary implant stability. (**c**) Cortical fracture observed in specimen 6, in which primary implant stability was maintained.

In one specimen, the cortical fracture resulted in rotational mobility and loss of primary stability, and the implant was classified as unsuccessful. In the second specimen, primary stability was maintained despite the cortical fracture.

The unstable implant was placed in a zygomatic bone with a volume of 2.69 cm^3, one of the smallest volumes observed in the study. However, because only two cortical fractures occurred, the study was not powered to determine whether reduced zygomatic bone volume increased the risk of fracture.

No implant penetrated the orbital cavity or infratemporal fossa. No macroscopically identifiable injury to the infraorbital region was observed. No unintended facial soft-tissue perforation occurred when adequate tissue retraction was maintained. No other implant required removal or repositioning.

4. Discussion

The present study represents the second stage in the experimental validation of a novel reverse zygomatic implant system developed for patients in whom conventional intraoral insertion may be technically impossible because of severe trismus, extensive maxillary defects, or altered post-oncological anatomy. Whereas Part 1 introduced the implant prototype design, CT-based virtual workflow and established the technical feasibility of the reverse-insertion concept in a single cadaveric specimen [12]. The present investigation evaluated the reproducibility, positional accuracy, anatomical safety, and prosthetic correspondence of the complete protocol in an expanded series of nine fresh-frozen cadaveric heads with substantial anatomical variability. The achievement of primary stability in 35 of the 36 implants, corresponding to a technical success rate of 97.2%, supports the reproducibility of the procedure under controlled experimental conditions.

The clinical problem addressed by this technique is highly specific but relevant. Conventional zygomatic implants are inserted from the intraoral region toward the zygomatic bone and require sufficient mouth opening to accommodate long drills, implant carriers, and insertion instruments. This may not be possible in patients with severe post-radiotherapy trismus, extensive maxillectomy defects, scar contracture, or bulky soft-tissue reconstructions. Reverse insertion changes the direction of the surgical procedure by initiating drilling and implant placement at the external zygomatic surface and directing the

implant toward a prosthetically predetermined intraoral emergence point. The proposed technique is not intended to replace conventional zygomatic implant placement in routinely accessible maxillae. Instead, it may represent an alternative for a carefully selected subgroup of patients for whom conventional placement is technically impossible or carries an unacceptable risk because of limited intraoral access.

The reverse zygomatic implant concept was initially reported by Dawood et al., who used a reverse implant as part of the rehabilitation of a patient with a hemimaxillectomy [11]. However, that report described an individualized clinical solution rather than a standardized surgical system and did not provide a quantitative comparison between the virtually planned and achieved implant positions.

The reverse implant was designed to accommodate the anatomical and mechanical requirements associated with insertion from the zygomatic surface toward the oral cavity. Its active threaded segment was intended to obtain primary anchorage within the zygomatic bone, whereas the polished passive segment crossed the maxillary defect and emerged intraorally. This design differs from that of conventional zygomatic implants, which are inserted from the alveolar or palatal region and advanced toward the zygomatic body [11,12].

The active threaded segment was limited to the region expected to engage the zygomatic bone. Previous virtual anatomical studies have demonstrated considerable interindividual variability in zygomatic bone volume, intraosseous trajectory length, and spatial relationships with the maxillary sinus and orbital structures [15]. This variability was also evident in the present series, in which zygomatic bone volume ranged from 2.53 to 8.10 cm^3. These findings reinforce the need for individual CT segmentation and virtual planning rather than relying on a standardized implant length, entry point, or angulation.

Thirty-four of the 36 implant trajectories followed an extrasinusal pathway corresponding to ZAGA III or IV anatomy, and a mean of 68.6% of the planned implant trajectory was located outside the segmented zygomatic bone. This finding does not indicate inadequate planning, because only the active threaded portion of the reverse implant was intended to engage the zygoma. Nevertheless, the long extraosseous segment highlights the importance of controlling the relationship between the implant and the residual maxillary tissues, orbital boundaries, facial soft tissues, and intraoral prosthetic emergence point.

The reverse-insertion procedure also introduced specific technical requirements. In some specimens, additional preparation of the external zygomatic cortex was necessary to accommodate the diameter of the implant carrier. This suggests that the relationship among the carrier diameter, cortical osteotomy, drilling sequence, and implant geometry requires further refinement. Excessive cortical preparation could reduce the amount of bone available for mechanical anchorage, whereas insufficient preparation may increase insertion resistance and the risk of cortical fracture. Future versions of the system should therefore seek to minimize the dimensions of the carrier and optimize the drilling sequence while preserving sufficient cortical support.

The mean deviation at the zygomatic entry point was 2.22 mm, the mean intraoral emergence deviation was 4.41 mm, and the mean angular deviation was 3.83°. The greater deviation at the intraoral emergence point is geometrically plausible. Potential sources of error in the present workflow include CT acquisition, image segmentation, virtual implant positioning, manufacturing tolerances of the drilling guides, adaptation of the guide to the zygomatic surface, guide fixation, drill-to-sleeve tolerance, deflection of the long drills, cortical resistance, and deviation during final implant insertion. Although each individual source may produce only a limited discrepancy, their cumulative effect can become clinically relevant at the intraoral emergence point. Similar cumulative error patterns have been described in computer-guided implant surgery, particularly when long

drilling paths and multiple sequential components are involved [16]. In the context of zygomatic implant placement, computer-assisted planning and specimen-specific guides may improve trajectory control, although accurate guide adaptation and stable fixation remain essential [7].

No statistically significant differences were identified among implant positions 13, 15, 23, and 25. Posterior sites showed numerically greater intraoral and angular deviations, but these differences did not reach statistical significance. This suggests that accuracy was not determined exclusively by whether the implant was located in an anterior or posterior position. Instead, specimen-specific anatomy, guide adaptation, bone resistance, accessibility, and surgical manipulation may have contributed more substantially to the observed variability.

Similarly, no significant differences were detected between the right and left sides. Laterality could theoretically influence drilling control because of surgeon position, hand dominance, access, visibility, and instrument orientation. Nevertheless, the present results did not demonstrate a systematic laterality-related effect. The limited number of specimens means that small differences between sides cannot be definitively excluded.

The observed accuracy results should not automatically be considered clinically acceptable solely because most implants achieved primary stability. Surgical stability and prosthetic accuracy represent related but distinct outcomes. A deviation that does not compromise zygomatic anchorage may still alter the intraoral emergence position or abutment angulation sufficiently to interfere with passive prosthetic seating. Both surgical and prosthetic endpoints must therefore be evaluated before determining the clinical applicability of the technique.

Both the superior blepharoplasty approach and the inferior transconjunctival approach with lateral canthotomy and cantholysis provided sufficient exposure for drilling-guide positioning, osteotomy preparation, and reverse implant insertion. No statistically significant differences were identified between the approaches in terms of zygomatic, intraoral, or angular deviation.

This finding refines the preliminary observations reported in Part 1. In the initial proof-of-concept specimen, the superior approach showed smaller deviations and appeared to provide greater drilling control [12]. However, that observation was based on a single cadaveric specimen and could not distinguish a true effect of the surgical access route from side-specific anatomy, guide adaptation, or procedural variability. In the present expanded paired analysis, the apparent quantitative superiority of the superior approach was not reproduced.

The inferior transconjunctival approach was subjectively considered by both surgeons (C.M-P. and A.F.-F) to provide greater working space and easier positioning of the drilling guide in several specimens. Nevertheless, this qualitative surgical impression did not translate into statistically superior placement accuracy. Surgical exposure and quantitative precision should therefore be considered separately. An approach may facilitate guide insertion and instrument manipulation without necessarily reducing the final three-dimensional deviation.

The transconjunctival approach has been extensively used to access the zygomatic and orbital regions while avoiding a visible cutaneous scar [17,18]. However, living patients may exhibit bleeding, tissue tension, edema, scarring, altered eyelid support, and postoperative functional or aesthetic complications that cannot be reproduced in a cadaveric model. The selection of surgical access should ultimately consider not only implant accuracy but also previous scars, eyelid anatomy, soft-tissue thickness, the location of the planned zygomatic entry points, the presence of previous reconstructive procedures, and surgeon experience.

Therefore, the present findings support the technical feasibility of both surgical approaches but do not establish their clinical equivalence. Future clinical investigations should compare not only placement accuracy but also surgical duration, accessibility, postoperative edema, eyelid position, scar visibility, sensory disturbances, ocular symptoms, and patient satisfaction.

Two fractures of the anterior zygomatic cortical wall occurred during the placement of 36 implants, corresponding to 5.6% of all implant placements. One fracture resulted in rotational mobility and loss of primary stability, whereas the second implant retained stability. These complications indicate that successful reverse placement depends not only on the planned trajectory but also on local cortical thickness, zygomatic morphology, osteotomy preparation, implant diameter, insertion resistance, and the position of the active threaded segment [19].

The unsuccessful implant was placed in a zygomatic bone with a volume of 2.69 cm^3, one of the smallest volumes observed in the series. However, zygomatic bone volume was not significantly correlated with placement deviation, and only two fractures occurred. It is therefore not possible to infer that reduced total zygomatic bone volume was the cause of cortical fracture.

Total segmented volume may also be an incomplete surrogate for local bone quality and mechanical resistance. Cortical thickness, trabecular architecture, bone density, local curvature, the distance between the osteotomy and the zygomatic borders, and the amount of bone surrounding the active threaded portion may be more relevant determinants of primary stability than total bone volume alone [19].

The 5 mm diameter of the active threaded segment was intended to improve mechanical engagement within the zygomatic bone. However, increasing implant diameter does not necessarily improve safety in every anatomical configuration. Although a wider implant may increase the bone-to-implant contact area and potentially modify stress distribution, it also requires a larger osteotomy and leaves less residual bone surrounding the implant [19–21]. A patient-specific balance must therefore be achieved among implant diameter, cortical engagement, available zygomatic bone, and fracture risk.

Future studies should incorporate quantitative measurements of cortical thickness and radiological bone density along the planned implant trajectory. Recording insertion torque and implant stability quotient values would provide a more objective evaluation of primary stability than manual assessment alone. Mechanical testing under cyclic loading would also be necessary to determine whether implants that retain initial stability after a limited cortical fracture can withstand long-term functional forces.

The specimen-specific verification bar demonstrated complete correspondence with a median of two of the four transepithelial abutments per specimen. None of the nine verification bars achieved complete passive seating over all four abutments simultaneously. This finding is particularly relevant because it demonstrates that technical success in implant placement does not necessarily result in sufficient accuracy for direct connection of a prefabricated definitive full-arch framework.

The incomplete seating probably reflects the accumulation of linear and angular deviations across multiple implants. Even relatively limited discrepancies at individual implants can prevent passive seating when four abutments must be simultaneously engaged by a rigid structure. The prosthetic effect of these discrepancies may be amplified in a full-arch framework, where misfit can generate strain at the implant–abutment interface, loosening of prosthetic screws, material fatigue, fracture of prosthetic components, or increased stress within the supporting bone.

The present findings refine the preliminary prosthetic observations reported in Part 1, in which partial seating of the verification bar was considered compatible with subse-

quent fixed rehabilitation [12]. The expanded series indicates that a definitive prosthesis should not be manufactured solely from the preoperative virtual implant positions. Instead, the definitive prosthetic workflow should incorporate the actual postoperative implant positions.

Potential strategies include intraoperative or postoperative digital scanning, photogrammetry, splinted impression techniques, corrective multi-unit abutments, or fabrication of the definitive framework after implant placement. The use of individualized angulated abutments may also compensate for limited discrepancies in implant emergence or inclination, although the degree of correctable deviation must be established.

The verification bar employed in this study was an assessment tool rather than a definitive prosthesis. Partial mismatch does not demonstrate that fixed rehabilitation would be impossible. However, it shows that the current workflow cannot yet guarantee passive seating of a prefabricated four-implant framework. Further optimization of guide stability, drilling tolerances, implant transfer, abutment positioning, and intraoral emergence control is therefore required.

No implant penetrated the orbital cavity or infratemporal fossa, and no macroscopically identifiable injury to the infraorbital region was observed. No unintended facial soft-tissue perforation occurred, as adequate retraction was maintained. These findings support the anatomical feasibility of the specimen-specific guided workflow under the controlled conditions of the study. However, this does not necessarily imply demonstrated surgical safety in clinical practice.

Nevertheless, the absence of observed injury in nine cadaveric specimens should not be interpreted as demonstrating that orbital, neural, vascular, or soft-tissue complications are impossible. The proximity of the implant trajectory to these structures requires accurate three-dimensional planning and controlled positioning of the surgical guide. Direct visualization, adequate tissue retraction, stable guide fixation, and verification of the planned trajectory remain essential.

The reverse technique may complement existing reconstructive alternatives. Zygomatic implants placed during or after maxillectomy have been used to support obturators and fixed prostheses, including through computer-guided surgical protocols [6,7]. The zygomatic implant perforated flap technique (ZIP-flap technique) combines oncological resection, soft-tissue reconstruction, and implant-supported rehabilitation within a coordinated pathway and has demonstrated favorable patient-related outcomes in appropriately selected cases [22]. Patient-specific subperiosteal implants represent another potential option for patients with severe maxillary atrophy or complex post-resection anatomy [23,24].

However, these alternatives are not interchangeable. Immediate placement of zygomatic implants or ZIP-flap reconstruction generally requires integration with the oncological and reconstructive procedure. Secondary rehabilitation may be substantially more difficult in patients treated several years previously, particularly when only soft tissue is available, anatomical landmarks are distorted, and severe trismus prevents conventional implant insertion. It is in this restricted clinical context that reverse zygomatic implant placement may provide its greatest potential benefit.

Several limitations must be considered when interpreting the findings of this study.

First, this was an experimental cadaveric investigation and did not include living patients. Fresh-frozen specimens provide a realistic representation of osseous anatomy but cannot reproduce bleeding, tissue perfusion, edema, muscle tone, pain, healing, scar formation, infection, osseointegration, or postoperative eyelid function. The model also cannot fully reproduce the functional restriction associated with severe trismus.

Second, standardized Brown Class II maxillectomies were surgically created in specimens without the variable anatomical consequences of previous oncological treatment.

Clinical patients may present irregular resections, radiotherapy-related fibrosis, osteoradionecrosis, soft-tissue flaps, skin paddles, vascular pedicles, scar contracture, and substantial loss or displacement of anatomical landmarks. The experimental model may therefore be less complex than the clinical conditions for which the technique is intended.

Third, the limited sample of the study remained insufficient to detect uncommon complications, establish equivalence between the surgical approaches, or perform definitive subgroup analyses. The four implants placed within each specimen were also not statistically independent. Although specimen-level means and paired analyses were used where appropriate, residual clustering and limited statistical power must be acknowledged.

Fourth, primary stability was assessed intraoperatively but was not systematically quantified using insertion torque or resonance-frequency analysis. No histological evaluation was performed, and the study could not assess osseointegration, peri-implant tissue response, long-term stability, or functional loading.

Fifth, the accuracy analysis depended on CT segmentation and registration of the preoperative and postoperative datasets. Measurement error may have arisen from image resolution, metal artifacts, threshold selection, surface reconstruction, identification of the implant axes, and the registration procedure. Interobserver and intraobserver reliability of the measurements was not evaluated.

Sixth, the investigation assessed only one prototype implant system and one specific drilling-guide workflow. The need for additional cortical preparation in some specimens suggests that the dimensions of the implant carrier and the relationship between the instruments and implant design require further optimization. The present results cannot necessarily be extrapolated to other implant geometries, guide materials, or surgical instrumentation.

Seventh, potential operator and learning-curve effects were not specifically evaluated. The accuracy and complication profile may differ among surgeons depending on their experience in zygomatic implantology, orbital approaches, computer-assisted planning, and specimen-specific guided surgery.

Eighth, the study did not compare the guided reverse-insertion protocol with freehand surgery, dynamic navigation, or another control technique. Consequently, the specific contribution of the static drilling guides to accuracy and safety cannot be quantified from the present results.

Ninth, as prosthetic correspondence was assessed macroscopically using a polyamide verification bar, which exhibits slight flexibility, the analysis did not quantify three-dimensional prosthetic misfit, strain, or the force required to seat the bar. A definitive prosthesis was not fabricated, and neither immediate loading nor cyclic biomechanical testing was performed. Therefore, the study cannot determine whether the observed deviations would be compatible with long-term functional rehabilitation.

Finally, patient-centered clinical outcomes, including mastication, speech, oral hygiene, facial aesthetics, pain, quality of life, and satisfaction, could not be evaluated. Prospective clinical investigations with adequate follow-up will be required before the technique can be recommended for routine clinical use.

Further technical development should focus on improving the adaptation and fixation of the specimen-specific guides, reducing drill-to-sleeve and carrier tolerances, refining external cortical preparation, and optimizing control of the intraoral emergence point. Dynamic navigation or real-time tracking could potentially complement static guides by identifying deviations during drilling and implant insertion.

Future anatomical studies should quantify cortical thickness, bone density, and the amount of residual bone surrounding the active implant segment. Objective measurements of insertion torque and implant stability should be correlated with local anatomy and

implant geometry. Biomechanical studies should assess stress distribution, resistance to cyclic loading, and the effect of limited cortical fractures on long-term implant stability.

Before clinical application, the protocol should also include a validated prosthetic strategy based on the achieved postoperative implant positions rather than relying exclusively on the preoperative virtual plan. Carefully selected prospective clinical studies should subsequently evaluate surgical morbidity, orbital and eyelid outcomes, implant survival, osseointegration, prosthetic complications, hygiene accessibility, speech, mastication, and patient-reported quality of life.

5. Conclusions

Within the limitations of this cadaveric study, reverse zygomatic implant placement using CT-based virtual planning and specimen-specific surgical guides was technically feasible and reproducible regarding implant stability. However, prosthetic workflow success could not be determined in real-life conditions. At the moment the reverse zygomatic implant technique should still be considered an experimental alternative for carefully selected patients in whom conventional zygomatic implant placement is precluded by severe trismus or complex post-maxillectomy anatomy. Its clinical safety, osseointegration, prosthetic performance, and long-term functional outcomes must be established in prospective clinical studies before routine clinical implementation.

Author Contributions: Conceptualization, A.F.-F. and C.M.-P.; methodology, A.F.-F. and C.M.-P.; formal analysis, A.F.-F. and C.M.-P.; validation, A.F.-F. and C.M.-P.; software, A.F.-F. and C.M.-P.; investigation, A.F.-F. and C.M.-P.; resources, A.F.-F. and C.M.-P.; data curation, A.F.-F.; writing—original draft preparation, A.F.-F. and C.M.-P.; writing—review and editing, F.J.C.-G., R.S.-G., S.A.-H.-C., E.G.-D., A.P.-G., L.P.-A., P.R.-B. and I.V.-M.; visualization, A.F.-F.; supervision, C.M.-P.; project administration, C.M.-P.; funding acquisition, C.M.-P. All authors have read and agreed to the published version of the manuscript.

Funding: This study received no direct funding. However, Avinent (Santpedor, Spain) provided the materials (implants, guides and screws) used in this project.

Institutional Review Board Statement: This study was conducted on a fresh-frozen human cadaveric head under laboratory conditions reproducing clinical maxillofacial surgery standards. Ethical approval was obtained from the Bioethics Commision of the University of Barcelona (IRB00003099, date of approval: 28 February 2022), and all procedures conformed to the ethical principles of the Declaration of Helsinki (2013 revision) and relevant institutional anatomical donation regulations.

Informed Consent Statement: The cadaveric specimens used were provided by the University's Anatomy Laboratory. The donor had expressly bequeathed their body pre-mortem, signing a donor consent form that permits its use for both educational and research purposes.

Data Availability Statement: All data supporting the reported results can be found in the article.

Acknowledgments: The authors would like to thank Avinent for their technical support and for providing the materials necessary to develop the project. To Ermengol Coma Redon, for his statistical support. During the preparation of this manuscript, the authors used OpenAI (Gemini 3.1 Pro) to assist with the organization of the manuscript and to improve the clarity, readability, and linguistic quality of the text. The AI tool was not used to generate scientific data, perform statistical analyses, interpret the results, or formulate the scientific conclusions. Following the use of this tool, the authors carefully reviewed and edited the manuscript and take full responsibility for the accuracy, integrity, and content of the published article.

Conflicts of Interest: The authors acknowledge Avinent (Santpedor, Spain) for their in-kind support in providing materials and collaborating on surgical planning and the subsequent comparison of planned versus clinical outcomes. The funders played no role in the study design; the collection, analysis, or interpretation of data; the drafting of the manuscript; or the decision to publish the results.

No financial compensation was exchanged between the funders and the authors. The authors declare no other conflicts of interest.

References

1. Wijbenga, J.G.; Schepers, R.H.; Werker, P.M.N.; Witjes, M.J.H.; Dijkstra, P.U. A Systematic Review of Functional Outcome and Quality of Life Following Reconstruction of Maxillofacial Defects Using Vascularized Free Fibula Flaps and Dental Rehabilitation Reveals Poor Data Quality. *J. Plast. Reconstr. Aesthetic Surg.* **2016**, *69*, 1024–1036. [CrossRef]
2. Sato, N.; Koyama, S.; Mito, T.; Izumita, K.; Ishiko, R.; Yamauchi, K.; Miyashita, H.; Ogawa, T.; Kosaka, M.; Takahashi, T.; et al. Changes in Oral Health-Related Quality of Life after Oral Rehabilitation with Dental Implants in Patients Following Mandibular Tumor Resection. *J. Oral Sci.* **2019**, *61*, 406–411. [CrossRef]
3. Shirota, T.; Shimodaira, O.; Matsui, Y.; Hatori, M.; Shintani, S. Zygoma Implant-Supported Prosthetic Rehabilitation of a Patient with a Maxillary Defect. *Int. J. Oral Maxillofac. Surg.* **2011**, *40*, 113–117. [CrossRef]
4. Brånemark, P.; Gröndahl, K.; Öhrnell, L.; Nilsson, P.; Petruson, B.; Svensson, B.; Engstrand, P.; Nannmark, U. Zygoma Fixture in the Management of Advanced Atrophy of the Maxilla: Technique and Long-term Results. *Scand. J. Plast. Reconstr. Surg. Hand Surg.* **2004**, *38*, 70–85. [CrossRef]
5. Galve, A. Zygoma Quad Compared with 2 Zygomatic Implants—A Systematic Review and Meta-analysis. *Clin. Oral Implant. Res.* **2019**, *30*, 402. [CrossRef]
6. Pellegrino, G.; Tarsitano, A.; Basile, F.; Pizzigallo, A.; Marchetti, C. Computer-Aided Rehabilitation of Maxillary Oncological Defects Using Zygomatic Implants: A Defect-Based Classification. *J. Oral Maxillofac. Surg.* **2015**, *73*, 2446.e1–2446.e11. [CrossRef]
7. Vosselman, N.; Glas, H.H.; Merema, B.J.; Kraeima, J.; Reintsema, H.; Raghoebar, G.M.; Witjes, M.J.H.; De Visscher, S.A.H.J. Three-Dimensional Guided Zygomatic Implant Placement after Maxillectomy. *J. Pers. Med.* **2022**, *12*, 588. [CrossRef]
8. Vosselman, N.; Glas, H.H.; De Visscher, S.A.H.J.; Kraeima, J.; Merema, B.J.; Reintsema, H.; Raghoebar, G.M.; Witjes, M.J.H. Immediate Implant-Retained Prosthetic Obturation after Maxillectomy Based on Zygomatic Implant Placement by 3D-Guided Surgery: A Cadaver Study. *Int. J. Implant Dent.* **2021**, *7*, 54. [CrossRef]
9. Borges, M.; Malta, C.; Ribeiro, R.; Cetira-Filho, E.; De Moura, J.; Rebouças, L.; Costa, F.; Silva, P.; Mota, M. Chemotherapy Increases the Prevalence of Radiotherapy-Related Trismus in Head and Neck Cancer Patients: A Systematic Review and Meta-Analysis. *J. Clin. Exp. Dent.* **2024**, *16*, e503–e515. [CrossRef]
10. Agarwal, P.; Shiva Kumar, H.R.; Rai, K.K. Trismus in Oral Cancer Patients Undergoing Surgery and Radiotherapy. *J. Oral Biol. Craniofacial Res.* **2016**, *6*, S9–S13. [CrossRef]
11. Dawood, A.; Collier, J.; Darwood, A.; Tanner, S. The Reverse Zygomatic Implant: A New Implant for Maxillofacial Reconstruction. *Int. J. Oral Maxillofac. Implants* **2015**, *30*, 1405–1408. [CrossRef]
12. Ferrer-Fuertes, A.; Cuesta-González, F.J.; Sieira-Gil, R.; Prats-Galino, A.; Aboul-Hosn-Centenero, S.; García-Díez, E.; Pozuelo-Arquimbau, L.; Rodriguez-Berart, P.; Vila-Masana, I.; AlOmari, B.; et al. A Novel Reverse Zygomatic Implant Approach: Step-by-Step Protocol and Cadaveric Validation for Trismus and Maxillectomy Sequelae—Part 1. *Prosthesis* **2026**, *8*, 39. [CrossRef]
13. Brown, J.S.; Rogers, S.N.; McNally, D.N.; Boyle, M. A Modified Classification for the Maxillectomy Defect. *Head Neck* **2000**, *22*, 17–26. [CrossRef]
14. Aparicio, C. A Proposed Classification for Zygomatic Implant Patients Based on the Zygoma Anatomy Guided Approach (ZAGA): A Cross-Sectional Survey. *Eur. J. Oral Implantol.* **2011**, *4*, 269–275. [PubMed]
15. Bertos Quílez, J.; Guijarro-Martínez, R.; Aboul-Hosn Centenero, S.; Hernández-Alfaro, F. Virtual Quad Zygoma Implant Placement Using Cone Beam Computed Tomography: Sufficiency of Malar Bone Volume, Intraosseous Implant Length, and Relationship to the Sinus According to the Degree of Alveolar Bone Atrophy. *Int. J. Oral Maxillofac. Surg.* **2018**, *47*, 252–261. [CrossRef]
16. Vercruyssen, M.; Cox, C.; Coucke, W.; Naert, I.; Jacobs, R.; Quirynen, M. A Randomized Clinical Trial Comparing Guided Implant Surgery (Bone- or Mucosa-supported) with Mental Navigation or the Use of a Pilot-drill Template. *J. Clin. Periodontol.* **2014**, *41*, 717–723. [CrossRef]
17. Uemura, T.; Watanabe, H.; Masumoto, K.; Chuman, T.; Satake, Y.; Yanai, T.; Harada, Y.; Ishihara, Y.; Kikuchi, M. Transconjunctival Approach for Zygomatic Fracture: A Single Surgeon's Experience of More Than 20 Years. *Plast. Reconstr. Surg. Glob. Open* **2016**, *4*, e757. [CrossRef]
18. Mombaerts, I.; Allen, R.C. The Transconjunctival Orbitotomy: A Versatile Approach to the Orbit and Beyond. *Surv. Ophthalmol.* **2023**, *68*, 265–279. [CrossRef]
19. Barausse, C.; Felice, P.; Pistilli, R.; Pellegrino, G.; Bonifazi, L.; Tayeb, S.; Fazio, A.; Marvi, M.V.; Manzoli, L.; Ratti, S. Anatomical Measurements of the Malar Bone for Safe Zygomatic Implant Placement: A Study on Donated Bodies. *J. Clin. Med.* **2024**, *13*, 6798. [CrossRef]
20. Korkmaz, F.M.; Korkmaz, Y.T.; Yaluğ, S.; Korkmaz, T. Impact of Dental and Zygomatic Implants on Stress Distribution in Maxillary Defects: A 3-Dimensional Finite Element Analysis Study. *J. Oral Implantol.* **2012**, *38*, 557–567. [CrossRef]

21. Tezerişener, H.A.; Özalp, Ö.; Altay, M.A.; Sindel, A. Comparison of Stress Distribution around All-on-Four Implants of Different Angulations and Zygoma Implants: A 7-Model Finite Element Analysis. *BMC Oral Health* **2024**, *24*, 176. [CrossRef]
22. Butterworth, C.J.; Rogers, S.N. The Zygomatic Implant Perforated (ZIP) Flap: A New Technique for Combined Surgical Reconstruction and Rapid Fixed Dental Rehabilitation Following Low-Level Maxillectomy. *Int. J. Implant Dent.* **2017**, *3*, 37. [CrossRef]
23. Mommaerts, M.Y. Additively Manufactured Sub-Periosteal Jaw Implants. *Int. J. Oral Maxillofac. Surg.* **2017**, *46*, 938–940. [CrossRef]
24. Gellrich, N.-C.; Korn, P.; Jehn, P.; Neuhaus, M.; Lentge, F.; Rahlf, B. Exceptional Cases Demand Exceptional Personalized Solutions: The Next Level in Dental Rehabilitation. *J. Pers. Med.* **2024**, *14*, 294. [CrossRef]

Disclaimer/Publisher's Note: The statements, opinions and data contained in all publications are solely those of the individual author(s) and contributor(s) and not of MDPI and/or the editor(s). MDPI and/or the editor(s) disclaim responsibility for any injury to people or property resulting from any ideas, methods, instructions or products referred to in the content.